





REGULAR ARTICLE

Optimization of Defect Detection in Atomic Materials Using Graphene Layer

Sonal C. Bhangale^{1,*} , Laxmikant S. Dhamande², Bhagyashree Ashok Tingare³, Tarun Dhar Diwan⁴,
R.A. Kapgate¹, P. William⁵ , Prasad M. Patore²

¹ Department of Mechatronics Engineering, Sanjivani College of Engineering, Kopergaon, MH, India

² Department of Mechanical Engineering, Sanjivani College of Engineering, Kopergaon, MH, India

³ Department of Artificial Intelligence and Data Science, D Y Patil College of Engineering, Akurdi, Pune

⁴ Contoller of Examination (COE), Atal Bihari Vajpayee University, Bilaspur, India

⁵ Department of Information Technology, Sanjivani College of Engineering, Kopergaon, MH, India

(Received 03 April 2025; revised manuscript received 18 August 2025; published online 29 August 2025)

The qualities of graphene and other atomic materials, coupled with computer vision methods, enable radical improvements in the sensitivity of flaw detection. The data collection process obtained in the methods was high-resolution imaging which applied to capture minute surface details of the atomic materials. The photos are exposed to contemporary feature extraction techniques to highlight and improve the details of the main structural components after undergoing stringent data pretreatment stages like noise reduction and picture standardization. The unique Effective Chicken Swarm Guided Recursive NeuroNet (ECS-RNN) model aims to classify and detect defects by applying smart swarms and deep learning. Trained on the performance metrics achieved in this study, which indicates its capability of producing very high accurate and reliable predictions of 97.3 % F1-score, 98.5 % accuracy and 96.8 % precision. These results indicate advancement in defect detection using the proposed technique and show applicability of machine learning practices in solving very complex problems. The ECS-RNN model reveals substantial improvements in neural network computations, demonstrates its ability to retrieve relevant architectures with minimal erosion, which is advantageous in scenarios where the retrieval of crucial information is of utmost importance.

Keywords: Graphene layer, Atomic structure, Effective Chicken Swarm Guided Recursive NeuroNet (ECS-RNN), Median and wiener filter.

DOI: [10.21272/jnep.17\(4\).04028](https://doi.org/10.21272/jnep.17(4).04028)

PACS numbers: 68.37.Ps, 68.65.Pq

1. INTRODUCTION

The fact that a few elements can create various elemental mixtures and microstructures is fascinating from a chemical standpoint. Reflecting on the evolution of human, they constantly dedicate ourselves to controlling the structure of materials. To create weapons, the prehistoric man first polished the precious stones [1]. The modification that can be made advanced from the macro framework to the small and even to the atomic level after a long period of material development. Pristine crystals can be used to describe everything of solid-state physics and science of materials only becomes involved when genuine material qualities need to be defined in terms of flaws [2]. Effective, contemporary renewable energy storing and conversion techniques, including solar panels, splitting of water, hydrogen fuel cell batteries, and super capacitors have been made possible by the development and design of materials at the nanoscale. The secret to obtaining better efficiency and long-term reliability from

these devices lies not only developing new materials but also improving their structure and interaction characteristics [3]. Since it enables the deposit of pinhole-free sheets with atom-level control over density and formulation over surfaces that have elevated aspect ratios, atomic layer deposition (ALD) has emerged as a crucial technique for nanotechnology. Microstructure is a collection of all unstable lattice imperfections in a material [4]. Examples include mesoscopic defects like second-phase precipitation, planar defects like boundaries and mounting faults, line defects like displacements, and point defects like substitutional and interconnected atoms and voids. The regularity of the normally regular crystalline structure is broken by these kinds of lattice flaws, which are defined according to their structural characteristics [5]. According to the latest nanoscale analytic inquiry, their chemical characteristics are significant and distinctive. Both the electrical and thermal transport capabilities of thermoelectric substances can be strongly influenced by the arrangement of the defects as well as

* Correspondence e-mail: bhangalesonalmk@sanjivani.org.in



their particular chemical makeup, or their chemical embellishment state [6]. With quickly developing applications across atomic, graphical, spectrum, and text-based techniques, deep learning (DL) constitutes one of the key data science subjects with the quickest rate of growth. DL makes it possible to automatically identify characteristics and analyze unstructured material. The use of DL techniques in atomistic predicting has been spurred by the recent growth of huge materials databases. On the other contrary, improvements in image and spectrum data have mostly benefited from data manipulation made possible by generating unregulated DL techniques and high-quality forwarding models [7]. The main objective of the study is to improve defect identification in atomic materials by developing a computer vision approach. The work intends to increase the precision of structural anomaly identification by utilizing cutting-edge imaging techniques.

2. RELATED WORKS

With reference to [8], investigated how single atomic faults in monolayer WS₂ can cause electrically driven photon emission, and establish a direct correlation between the emission and the surrounding atom and electronic properties. An effective substrate for electrically driven, widely adjustable, atomic-scale single-photon generators were provided by inflexible charged carrier insertion into localized states of defect of two-dimensional substances.

The method for sub-picometer accuracy single-atom defects probing in a single-layer 2D transition metallic dichalcogenide was explained in [9]. Identified and categorized point flaws by using deep learning to explore massive datasets of aberration-corrected images. These findings suggest that computer vision could have an influence on the advancement of high-precision microscopy using electrons techniques for materials that were sensitive to beams.

To address laccase's intrinsic flaws, an initial iron single-atom anchoring N-doped carbon substance (Fe1@CN-20) was revealed as a laccase substitute in [10]. Furthermore, it can be utilized at least seven times with a minor decrease in functionality. Therefore, compared to laccase, which has been used in the recognition and destruction of a number of phenolic compounds, this material is significantly less expensive and has better stability and recycling ability.

According to the author of [3, 11], the localized chemically decorating states of different kinds of lattice faults in thermoelectric substances were investigated and the findings were obtained using atom probe tomography (APT). To help direct the rational development of outstanding performance thermoelectric substances, APT extends the idea of engineering defects to the realm of separation engineering, enabling a deeper understanding of the interaction between piezoelectric characteristics and microstructural characteristics.

3. METHODS AND MATERIALS

In this method, the faults or anomalies of atomic structure is evaluated by the collection of dataset, which involves SEM and AFM. To remove noise median and wiener filter could be effectively utilized for preprocessing and gray level co-occurrence matrix (GLCM) is implemented for future extraction. The proposed Effective Chicken swarm Guided Recursive NeuroNet (ECS-RNN) method can be effective determine the defect as shown in Fig. 1.

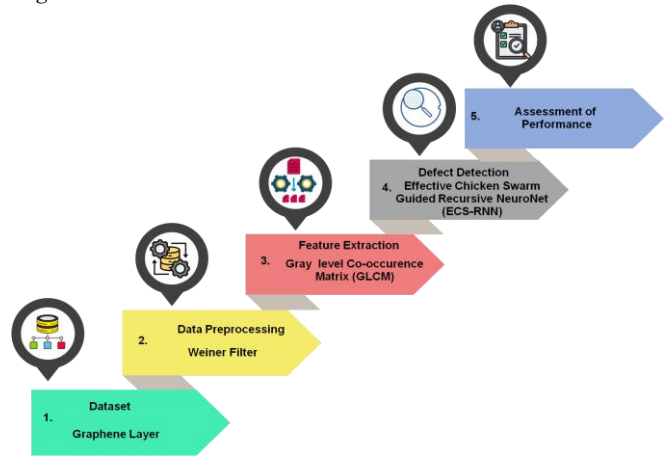


Fig. 1 – Schematic view of method flow incorporated in the study

3.1 Data collection

A dataset could consist of images with high resolution or scanning the image of graphene layers produced using advanced imaging techniques like AFM and SEM. The images have revealed a number of faults or anomalies in the atomic structure of the graphene, including as empty spaces, grain boundaries, displacements, and other surface imperfections. To train a computer vision model for defect recognition, marked specimens of both defective and non-faulty areas have been added to the dataset.

3.2 Data Preprocessing Using Median and Wiener Filters

By improving images quality, median and wiener filtering are essential preprocessing tools for fault identification in graphene layers. Typically, a suitable method, both median and wiener filtering is used to repair damaged images that are susceptible to noise. This could be stated mathematically as follows in Equations (1) and (2):

$$h(w, z) = e(w, z) * v(w, z) + m(w, z) \quad (1)$$

$$g(w, z) = Q[q(w, z)] \quad (2)$$

In this case, $e(w, z)$ indicates the obtained image, $v(w, z)$ is the deterioration function, $*$ indicates convolution, $m(w, z)$ stands for noise, including Gaussian fluctuations, $h(w, z)$ is the resultant deteriorated image, and $g(w, z)$ is the last result images after the method Q has been applied. To create de-noised images, the wiener and

median filters for noise reducing with quadratic temporal ranges are frequently employed. The following steps can help to improve the quality of images: Initially, a $m \times n$ mask matrix is established for the three-dimensional sound cancellation filter. After that, the filter medium is employed to evaluate the deteriorating image's newfangled region dimension, which matches its mask pixel size, in relation to the covered pixel frequency. The Wiener filter is expressed as follows and incorporates both the variation in and mean pixel values in the $m \times n$ sized mask matrix:

$$\mu = \frac{1}{MN} \sum_{m,n \in \eta} b(m,n) \quad (3)$$

$$\sigma^2 = \frac{1}{MN} \sum_{m,n \in \eta} b^2(m,n) - \mu^2 \quad (4)$$

Where in $a_x(n,m)$ stands for each pixel in the surrounding area η in the mask, $m \times n$ is the dimension of the surrounding area h , μ is the median, and σ^2 is the variability of the gaussian distortion in the images. The predicted values are used to convey the wiener filter to the additional region, which are denoted as $a_x(n,m)$. When the median and wiener filters are applied together for graphene layer defect detection, the noise level is significantly reduced. The Wiener filter adjusts to local variants, maintaining fine structural details and defects, while the median filter successfully removes salt-and-pepper noise without obscuring important features. This results in greater clarity, more reliable images for accurate defect identification.

3.3 Gray Level Co-Occurrence Matrix (GLCM) for Feature Extraction

To detect flaws like damage or gaps in graphene, GLCM measures the spatial correlations between pixel pairs and improves quality control analysis. Given a spatial relationship between the regions in a pattern, such an array displays the combined arrangement of gray intensity pairings of neighboring pixels. The three-dimensional connection of a distinct direction or distance among pixels yields matrices with distinct information. The co-occurrence matrix's column and row counts are solely determined by the pattern's gray values; the image size has no bearing. The amount of transition across gray levels m and n appearing in the texture based on a certain spatial connection is indicated by a component $O(n,m)$ of co-occurrence matrices. Prior to calculating the co-occurrence matrices, the sequence of pixels wherein the phases will be taken into consideration must be defined. S is constructed. Every pair of regulates for every pixel in the relationship makes up this set. Equation (6) serves for calculating the number of transitions among every pair of gray levels in the surface, once S has been specified. The gray value of a pixel in the image at (n,m) is indicated by the equation (6) can be written as:

$$O(n,m) = \{(j,i), (l,k)\} \in T | e(j,i) = n \text{ and } e(l,k) = m\} \quad (6)$$

After calculating the occurrence for every gray level

transition, $O(n,m)$ is positioned in the matrix's n -throw as well as m -th column. Following a standardization using Equation (7), wherein G_h represents the greatest gray level, descriptors of features are then obtained:

$$O_{n,m} = \frac{O(n,m)}{\sum_{j=0}^{G_h} \sum_{i=0}^{G_h} O(j,i)}, n, m = 0, \dots, G_h \quad (7)$$

The co-occurrence matrix is dependent upon the gray level transitions among pixel pairings in set, as per Equation (9). In this manner, both the angle and the distance among the pairings could be freely specified. Fast, non-invasive graphene quality assessment is made possible by this technique, which is essential for uses requiring excellent material integrity, such as nanotechnology and electronic devices.

3.4 Defect Detection Using Effective Chicken Swarm Guided Recursive NeuroNet (ECS-RNN)

The hybridized method of chicken swarm optimization and recursive neural network integrate cutting-edge deep learning methods with nature-inspired optimization to discover defects in layers of grapheme. This method improves detection efficiency and accuracy, which makes it helpful for spotting minute structural irregularities in graphene superior resolution electron microscopy images.

1.1.1 Recursive Neural Network (RNN)

Through the analysis of hierarchical data structures, RNN provide an efficient method for finding flaws in graphene layers. The intricate and recursive linkages seen in atomic and molecular structures are captured by RNNs, which enables them to identify anomalies. With vectors of characteristics, let \tilde{z}_i symbolize the combined result of a pattern's vector illustration in a layer. The sub-node phrase of the recall gates have two recall barriers for every pair for any node i . Considering using a binary tree, the dimension, which is the collection of variables from a pair of nodes i , is 2. A continuous dropout functional is $\text{drop}(w)$ in Equation (15). The RNN for every pattern to the real valued vector can be written as follows in the Equation (8):

$$\tilde{g}_i = \sum_{l \in A(i)} g_l \quad (8)$$

$$j_i = \sigma(X^j[w_i, \tilde{g}_i] + a^j) \quad (9)$$

$$e_{il} = \sigma(X^e[w_i, g_l] + a^e) \quad (10)$$

$$p_i = \sigma(X^p[w_i, \tilde{g}_i] + a^p) \quad (11)$$

$$v_i = \tanh(X^v[w_i, \tilde{g}_i] + a^v) \quad (12)$$

$$d_i = j_i \odot \text{drop}(v_i) + \sum_{l \in A(i)} e_{il} \odot d_l \quad (13)$$

$$g_i = p_i \odot \text{drop}(d_i) \quad (14)$$

$$\text{drop}(w) = \begin{cases} \max^* w & \text{if train phase;} \\ w, & \text{otherwise} \end{cases} \quad (15)$$

In Equations (16) and (17), employ an entirely connected layer as the resultant layer. Two for detection

and five for type classifiers are the number of classes that make up the entire layer's output size. For a given output, select the anticipated label \hat{z}_i at each *node* i . The cost function found in Equation (18) is computed using the softmax entropy cross classifier. The training set's total component count is denoted by z . The detection classifier's loss function changes to give the positive examples a three-fold higher loss than the negative cases to address the issue of class inequalities as shown below:

$$\hat{o}(z/w_i) = X^{(ed)} g_i + a^{(ed)} \quad (16)$$

$$\hat{z} = \underset{z}{\text{arg max}} \hat{o}(z, w_i) \quad (17)$$

$$I(\theta) = \frac{1}{n} \sum_i^n z^i \log(\text{softmax}(\hat{o}(\frac{z^i}{w}))) \quad (18)$$

RNNs, can handle multi-scale characteristics inside the graphene layer by recursively organizing data, which is essential for spotting minute, subtle fault structures that conventional techniques can overlook. RNNs improve detection effectiveness and precision, which makes them to ideal for continuous tracking in applications, including quality assurance and graphene fabrication.

4. RESULT

In this study, implementing Python 3.10 with Windows 10's system setup. When it comes to identifying atomic-level flaws, AFM performed better than SEM in terms of accuracy, precision, and recall. AFM proved its efficacy in atomic defect analysis by exhibiting better performance, especially in detecting pointed imperfections, structure warping, and lattice deformations, with improved precision and recall levels among various anomalies types.

4.1 Observation of Atomic Force Microscopy (AFM)

AFM, or atomic force microscopy, Table 1 and Fig. 2 shown remarkable efficacy in identifying a variety of flaws when used to analyze atomic structural abnormalities of the proposed model (ECS-RNN). With a F1 value of 96.7 % and mAP of 94.2 %, gaps were found with the greatest accuracy. With a mAP of 91.6 % and a F1 index of 95.3 %, dislocations came in second. The identification of the surface texture showed comparable superior accuracy, with a mAP of 92.5 % and a F1 index of 96.5 %. With a F1 value of 96.1 % and a mAP of 93.7 %, the identification of structural defects demonstrated a strong overall performance, demonstrating the efficiency of SEM in precisely detecting and describing atomic-level structural anomalies.

Table 1 – Characterization of atomic material defects using F1 score and map

Irregularity Type	F1 Score (%)	mAP (%)
Voids	96.7	94.2
Dislocations	95.3	91.6
Surface Roughness	96.5	92.5
Structural Defects (Overall)	96.1	93.7

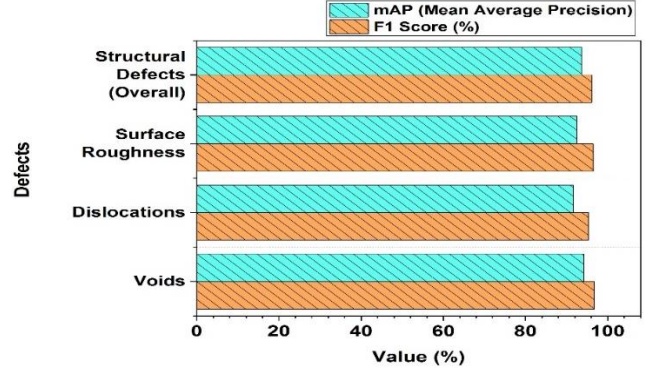


Fig. 2 – AFM-based microscopic surface features

4.2 SEM-Based Surface Topography Analysis

Numerous defect forms, including as gaps, displacements, rough surfaces, and atomic flaw localizations, were discovered through the application of SEM to analyze atomic structural anomalies as shown in the Table 2 and Fig. 3. High performance was shown in the identification of these abnormalities, with mean Average Precision (mAP) levels among 92.5 and 94.2 and F1 scores around 96.5 and 96.1. In particular, voids exhibited mAP of 94.2 and F1 score of 97.3, whereas rough surfaces and displacements had mAP measurements of 91.6 and 92.5, respectively, with F1 values of 95.3 and 96.5. With a F1 value of 96.1 and mAP of 93.7, atomic defect localizations had the greatest detection performance, demonstrating the excellent accuracy and dependability of SEM in detecting and describing atomic-scale defects.

Table 2 – Graphene SEM image detection and classification effectiveness for atomic defects

Irregularity Type	F1 Score (%)	mAP (%)
Voids	97.3	94.2
Dislocations	95.3	91.6
Surface Roughness	96.5	92.5
Atomic Defect Localizations	96.1	93.7

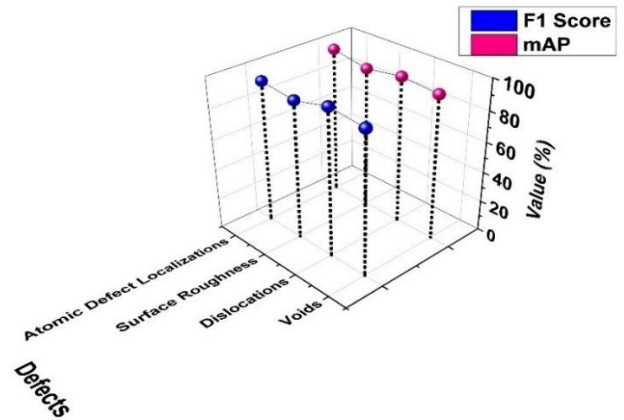


Fig. 3 – Examination of surface morphology by SEM

The suggested ECS-RNN model's metrics of performance for identifying different kinds of flaws. All fault categories show remarkable outcomes from the algorithm. For Voids, it attains a mAP of 96.5 %, an excellent F1 score of 94.9 %, recall of 95.6 %, precision of 94.9 %, and accuracy of 96.2 %. Although its mAP is 95.1 %, ECS-RNN performs slightly higher in the identification of dislocations, with accuracy of 97.3 %, precision of 95.5 %, F1 score of 96.2 % and recall of 96.8 %. While the mAP lowers to 94.2 %, Surface Roughness is also recognized precisely, with an F1 score of 95.3 %, precision of 96.5 %, accuracy of 95.6 %, and recall of 97.5 %. The model's mAP is little lower at 95.9 %, but generally it does exceptionally well in detecting structural defects, with the greatest accuracy of 98.5 %, precision of 97.2 %, recall of 96.5 %, and F1 score of 98.1 %. These outcomes show the ECS-RNN's excellent performance in a range of fault types.

REFERENCES

1. J. Yang, W. Li, D. Wang, Y. Li, *Small Struct.* **2** No 2, 2000051 (2021).
2. B. Gupta, M.A. Hossain, A. Riaz, A. Sharma, D. Zhang, H.H. Tan, C. Jagadish, K. Catchpole, B. Hoex, S. Karuturi, *Adv. Funct. Mater.* **32** No 3, 2109105 (2022).
3. Y. Yu, C. Zhou, S. Zhang, M. Zhu, M. Wuttig, C. Scheu, D. Raabe, G.J. Snyder, B. Gault, O. Cojocaru-Mirédin, *Mater. Today* **32**, 260 (2020).
4. K. Choudhary, B. DeCost, C. Chen, A. Jain, F. Tavazza, R. Cohn, C.W. Park, A. Choudhary, A. Agrawal, S.J. Billinge, E. Holm, *npj Comput. Mater.* **8** No 1, 59 (2022).
5. V. Gupta, K. Choudhary, F. Tavazza, C. Campbell, W.K. Liao, A. Choudhary, A. Agrawal, *Nat. Commun.* **12** No 1, 6595 (2021).
6. Y. Yu, M. Cagnoni, O. Cojocaru-Mirédin, M. Wuttig, *Adv. Funct. Mater.* **30** No 8, 1904862 (2020).
7. X. Meng, *J. Mater. Res.* **36**, 2 (2021).
8. B. Schuler, K.A. Cochrane, C. Kastl, E.S. Barnard, E. Wong, N.J. Borys, A.M. Schwartzberg, D.F. Ogletree, F.J.G. de Abajo, A. Weber-Bargioni, *Sci. Adv.* **6** No 38, eabb5988 (2020).
9. C.H. Lee, A. Khan, D. Luo, T.P. Santos, C. Shi, B.E. Janicek, S. Kang, W. Zhu, N.A. Sobh, A. Schleife, B.K. Clark, *Nano Lett.* **20** No 5, 3369 (2020).
10. Y. Lin, F. Wang, J. Yu, X. Zhang, G.P. Lu, *J. Hazard. Mater.* **425**, 127763 (2022).
11. F. Han, C. Cheng, J. Zhao, H. Wang, G. Zhao, Y. Zhang, N. Zhang, J. Zhang, Y. Wang, Q. Wei, *Colloid. Surf. B: Biointerface.* **242**, 114093 (2024).

5. CONCLUSION

Overall, the suggested method enhances neural network simulations with impressive outcomes. ECS-RNN's 98.5 % accuracy, 98.1 % F1-score, and 97.2 % precision demonstrate how well it produces reliable and accurate predictions. Its outstanding recall of 96.5 % further demonstrates its ability to detect relevant patterns with minimal loss. These findings establish that ECS-RNN significantly enriches the performance of models and offers a workable solution for difficult machine learning problems with optimization. The ECS-RNN method's dependence on certain datasets for testing may restrict its applicability to a variety of real-world scenarios. To improve ECS-RNN's resilience and generalization, future research could focus on applying it to larger datasets in a variety of fields.

Оптимізація виявлення дефектів в атомних матеріалах з використанням графенового шару

Sonal C. Bhangale¹, Laxmikant S. Dhamande², Bhagyashree Ashok Tingare³, Tarun Dhar Diwan⁴,
R.A. Kapgate¹, P. William⁵, Prasad M. Patare²

¹ Department of Mechatronics Engineering, Sanjivani College of Engineering, Kopergaon, MH, India

² Department of Mechanical Engineering, Sanjivani College of Engineering, Kopergaon, MH, India

³ Department of Artificial Intelligence and Data Science, D Y Patil College of Engineering, Akurdi, Pune

⁴ Controller of Examination (COE), Atal Bihari Vajpayee University, Bilaspur, India

⁵ Department of Information Technology, Sanjivani College of Engineering, Kopergaon, MH, India

Властивості графену та інших атомних матеріалів у поєднанні з методами комп'ютерного зору дозволяють радикально покращити чутливість дефектоскопії. Процес збору даних, отриманий за допомогою цих методів, включав зображення високої роздільної здатності, які застосовувалися для захоплення дрібних деталей поверхні атомних матеріалів. Фотографії піддаються сучасним методам вилучення ознак, щоб виділити та покращити деталі основних структурних компонентів після проходження суворих етапів попередньої обробки даних, таких як зменшення шуму та стандартизація зображення. Унікальна модель Effective Chicken Swarm Guided Recursive NeuroNet (ECS-RNN) спрямована на класифікацію та виявлення дефектів за допомогою застосування інтелектуальних роїв та глибокого навчання. Навчання проводилося на основі показників продуктивності, досягнутих у цьому дослідженні, що вказує на її здатність створювати дуже точні та надійні прогнози з показником F1 97,3 %, точністю 98,5 % та прецизійністю 96,8 %. Ці результати свідчать про прогрес у виявленні дефектів за допомогою запропонованої методики та демонструють застосовність методів машинного навчання у вирішенні дуже складних задач. Модель ECS-RNN демонструє суттєві покращення в обчисленнях нейронних мереж, демонструє свою здатність отримувати відповідні архітектури з мінімальною ерозією, що є перевагою в сценаріях, де отримання важливої інформації має першорядне значення.

Ключові слова: Шар графену, Атомна структура, Ефективна рекурсивна нейромережа, Керована методом Chicken Swarm (ECS-RNN), Медіанний та вінерський фільтри.